ACS Catalysis

Research Article

pubs.acs.org/acscatalysis

Methanolysis of Ammonia Borane by CoPd Nanoparticles

Daohua Sun,*[,†,‡] Vismadeb Mazumder,[‡] Önder Metin,[§] and Shouheng Sun*[,‡]

[†]Department of Chemical and Biochemical Engineering, College of Chemistry and Chemical Engineering, Xiamen University, Xiamen 361005, China

[‡]Department of Chemistry, Brown University, Providence, Rhode Island 02912, United States

[§]Department of Chemistry, Faculty of Science, Atatürk University 25240, Erzurum, Turkey

ABSTRACT: Monodisperse 7 nm CoPd nanoparticles (NPs) with controlled compositions were synthesized and studied for their catalyzing methanolysis of ammonia borane (AB). The NPs were prepared by the reduction of cobalt(II) acetylacetonate and palladium(II) bromide in the presence of oleylamine and trioctylphosphine. Deposited on a carbon support without any specific surface treatment, these NPs were active catalysts for methanolysis of AB, and their activities were composition-dependent. Among all CoPd catalysts tested, $Co_{48}Pd_{52}$ NPs exhibited the highest catalytic activity and stability. Kinetic study showed that the catalytic methanolysis of AB was first-order with respect to catalyst concentration and zero-order with respect to AB concentration. The activation energy for the methanolysis was calculated to be 25.5 kJ mol^{-1}. These CoPd NPs are a promising catalyst for AB methanolysis and for developing a highly efficient hydrogen generation system for power applications.

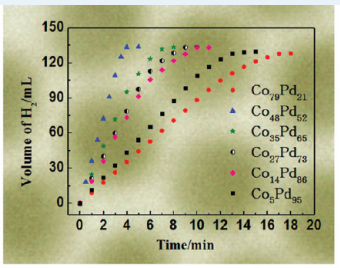

$H_3N{\bullet}BH_3 + 4\,CH_3OH \longrightarrow NH_4{\bullet}B(OCH_3)_4 + 3\,H_2$

KEYWORDS: *ammonia borane, methanolysis, bimetallic nanoparticles, cobalt−palladium alloy, hydrogen generation*

One of the most critical issues in hydrogen-based energy conversions is to store and release hydrogen under ambient conditions.[1,2] Ammonia−borane (H_3NBH_3, AB) has been studied extensively as a practical hydrogen storage material due to its high hydrogen capacity (19.6 wt %), high stability, and nontoxicity.[3−5] Hydrogen stored in AB can be released via solid state thermolysis, dehydrocoupling, hydrolysis, and methanolysis.[6] Among these releasing processes, AB hydrolysis in an aqueous solution is favored and well studied,[7−20] but the liberation of small quantity of ammonia at high AB concentrations in the presence of an active catalyst and inefficacy in recycling the hydrolysis product, ammonium metaborate (NH_4BO_2), can pose serious challenges to practical applications. On the other hand, methanolysis of AB appears to be advantageous for hydrogen generation. In the presence of a suitable catalyst, its complete reaction is as follows: $H_3N{\cdot}BH_3$ (aq) + $4CH_3OH \rightarrow NH_4{\cdot}B(OCH_3)_4 + 3H_2$ (g). Depending on the catalyst used, methanolysis reaction can even be initiated below 0 °C, thereby satisfying the applications in cold weather.[21] More importantly, the methanolysis product, $NH_4{\cdot}B(OCH_3)_4$, can be converted back to AB by room temperature reaction with $LiAlH_4$ in the presence of NH_4Cl.[22] The common catalysts tested for AB methanolysis are metal salts, including $RuCl_3$, $RhCl_3$, $CoCl_2$, $PdCl_2$, $NiCl_2$.[22] Because Ru and Rh salts show much higher activity than other transition metal salts, the supported Rh[23] and Ru[6,24] nanoclusters have also been developed so that the catalysts can be used and recycled; however, the Ru and Rh catalysts are too expensive to be applied as practical catalysts for AB methanolysis and for hydrogen generation.

Herein, we report the synthesis of 7 nm monodisperse alloy CoPd NPs with controlled compositions and evaluate their catalytic activity in hydrogen generation from the methanolysis of AB at room temperature. Recent research has indicated that bimetallic NPs containing a noble metal and a first-row transition metal have composition-dependent optical, magnetic, and catalytic properties that are different from any of the monometallic NP components.[24,25] With proper control on size, morphology, and compositions, their physical and chemical properties can be greatly enhanced.[26−28] Our recent study indicated that the alloy CoPd deposited on a carbon support (C) was, indeed, effective for accelerating the hydrolysis of AB, and its activity was comparable to Pt catalysts.[29] Here, we demonstrate that CoPd/C is also an efficient catalyst for the methanolysis of AB. Among the various CoPd NPs studied, $Co_{48}Pd_{52}$ NPs show the optimum activity and stability.

Monodisperse CoPd NPs were synthesized by high-temperature reduction of cobalt(II) acetylacetonate ($Co(acac)_2$) and palladium(II) bromide ($PdBr_2$) in the presence of oleylamine (OAm) and trioctylphosphine (TOP). In the reaction, TOP is likely to form a Co- and Pd-TOP cocomplex and promotes the

Received: March 29, 2012
Revised: May 14, 2012
Published: May 15, 2012

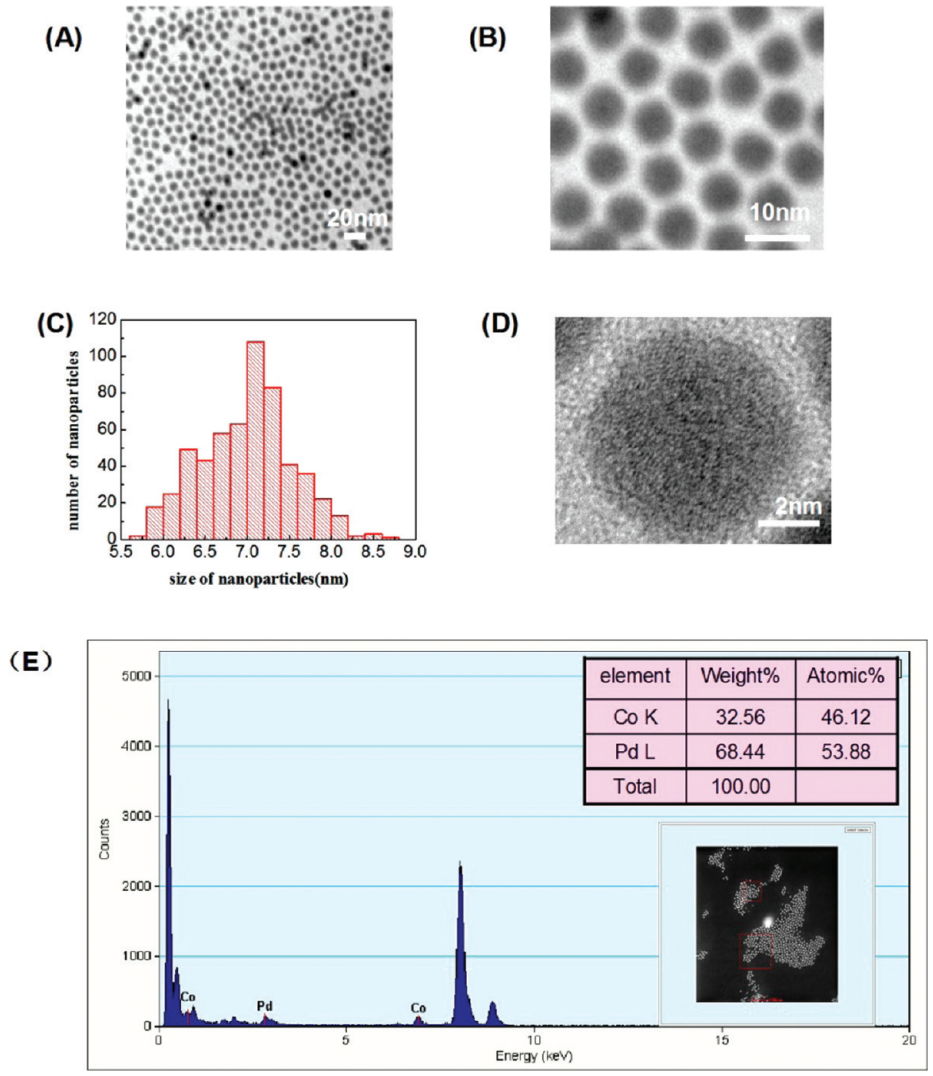

Figure 1. TEM images (A, B), histogram (C), HRTEM image (D), and EDX spectrum (E) of the 7 nm $Co_{48}Pd_{52}$ NPs formed from the reduction of the 0.35 mmol $Co(acac)_2$ and 0.15 mmol $PdBr_2$.

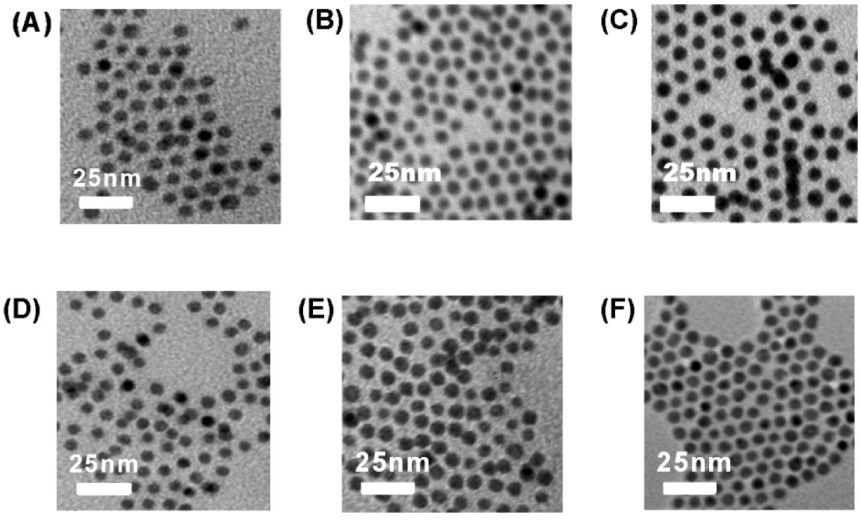

Figure 2. Representative TEM images of the CoPd NPs used for catalytic studies: (A) $Co_{79}Pd_{21}$, (B) $Co_{48}Pd_{52}$, (C) $Co_{35}Pd_{65}$, (D) $Co_{27}Pd_{73}$, (E) $Co_{14}Pd_{86}$, (F) Co_5Pd_{95}.

coreduction of Co and Pd salts.[30] Compositions of NPs were controlled by simply changing the metal salt ratios. For example, with metal salts at Co/Pd ratios of 4:1, 7:3, 3:2, 1:1, 2:3, and 1:4, $Co_{79}Pd_{21}$, $Co_{48}Pd_{52}$, $Co_{35}Pd_{65}$, $Co_{27}Pd_{73}$,

dx.doi.org/10.1021/cs300211y | ACS Catal. 2012, 2, 1290−1295

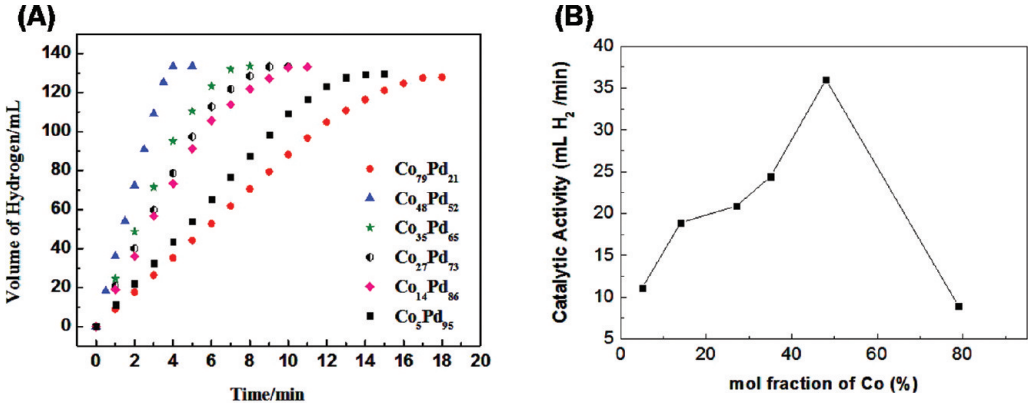

Figure 3. (A) Plot of time versus volume of hydrogen generated from methanolysis of AB catalyzed by different CoPd/C catalysts and (B) plot of catalytic activity versus mole fraction of cobalt (NP = 15 mg, [AB] = 200 mM, T = 25 ± 1 °C).

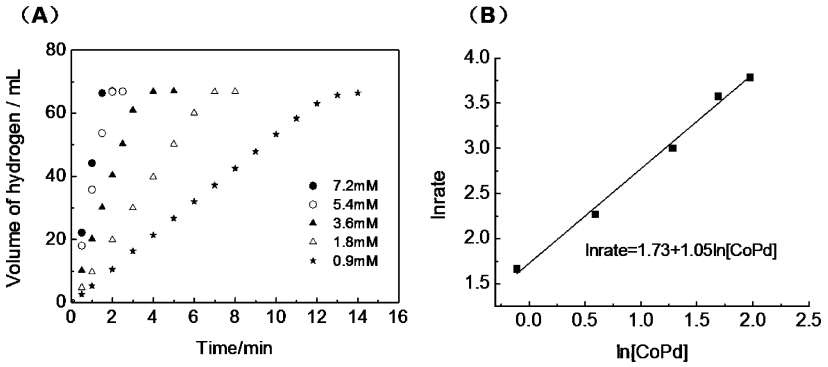

Figure 4. (A) Plot of time versus volume of hydrogen generated from methanolysis of AB catalyzed by $Co_{48}Pd_{52}$/C catalyst at different catalyst concentrations and (B) plot of hydrogen generation rate versus the catalyst concentration in logarithmic scale (rate = mL of H_2/min; [AB] = 100 mM, T = 25 ± 1 °C).

$Co_{14}Pd_{86}$, and Co_5Pd_{95} NPs, respectively, were obtained. In Figure 1, parts A and B show TEM images, and part C is the particle size histogram of the CoPd NPs of 7.0 ± 0.5 nm. HRTEM analysis on a representative single CoPd NP indicates that the as-synthesized CoPd NPs have a polycrystalline structure (part D). The polycrystalline structure of CoPd NPs could also be seen from their XRD pattern. An energy-dispersive X-ray (EDX) spectrum is given in part E, which proves the presence of Co and Pd elements at an atomic ratio of 46/54. The composition of the Co/Pd NPs was further analyzed by inductively coupled plasma-atomic emission spectroscopy (ICP–AES). The as-prepared 7 nm $Co_{48}Pd_{52}$ NPs contain 30 wt % of Co/Pd metals. Figure 2 displays more representative TEM images of the CoPd NPs used for catalytic evaluations. It can be seen that CoPd NPs with different compositions have no significant difference in either size or morphology.

The as-synthesized CoPd NPs (15.0 mg) with different compositions were deposited on Ketjen carbon support (45.0 mg) (25 wt % of NPs) and then mixed with a methanol solution of AB at room temperature. The volume of hydrogen gas generated was measured using the classic water-displacement method. Figure 3 plots the H_2 amount generated as a function of reaction time for every 10 mL of AB (2 mmol, 200 mM) methanol solution in the presence of 15 mg CoPd NPs. From these curves, we can see that when the 2 mmol of AB complex is completely reacted with methanol, 6 mmol H_2 (~134 mL) is generated. From the plot, we can also see that Co-rich ($Co_{79}Pd_{21}$) or Pd-rich (Co_5Pd_{95}) NPs show lower activity than the ones with a near equal Co/Pd ratio ($Co_{48}Pd_{52}$). Under our evaluation conditions, $Co_{48}Pd_{52}$ NPs/C catalyst is most active in catalyzing the AB methanolysis reaction with a completion time of 4 min and a total turnover frequency (TOF) value of 27.7 (mol of H_2·(mol of catalyst·min)$^{-1}$). The better catalytic activity of $Co_{48}Pd_{52}$ than Co-rich or Pd-rich NPs might be explained by the Sabatier principle, which states that optimal catalytic activity can be achieved on a catalytic surface with median binding energies of reactive intermediates.[31,32] Thus, it is believed that there is an optimal ratio between Co and Pd to show the highest catalytic activity in the methanolysis of AB.

The kinetics of AB methanolysis catalyzed by $Co_{48}Pd_{52}$ NPs was further studied under different catalyst concentrations, substrate concentrations, and temperatures. In a NP concentration-dependent methanolysis study, NP concentrations were controlled at 0.9, 1.8, 3.6, 5.4, and 7.2 mM (representing 2.5, 5.0, 10.0, 15.0, and 20.0 mg of $Co_{48}Pd_{52}$ NPs, respectively) while the initial AB concentration was kept at 100 mM. In AB concentration-dependent methanolysis, the NP concentration was kept at 5.4 mM while the AB concentrations were set at 50, 100, 150, 200, and 300 mM. To obtain the activation energy (E_a) of the catalytic methanolysis reaction, the methanolysis of AB (200 mM) was performed in the presence of 3.6 mM CoPd NPs at 15–40 °C. In all these tests, the gas product was analyzed by the acid–base titration method and showed no sign of ammonia, indicating that the gas generated during the reaction was pure H_2.

dx.doi.org/10.1021/cs300211y | ACS Catal. 2012, 2, 1290–1295

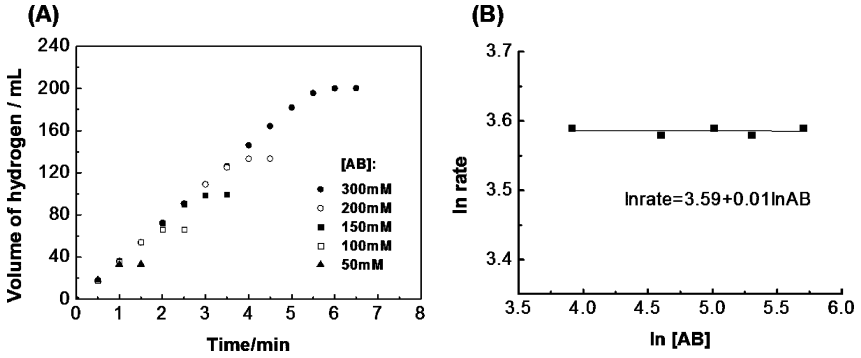

Figure 5. (A) Plot of time versus volume of hydrogen generated from methanolysis of AB catalyzed by $Co_{48}Pd_{52}/C$ catalyst at different AB concentrations and (B) plot of hydrogen generation rate versus the AB concentration in logarithmic scale (rate = mL of H_2/min; [CoPd] = 5.4 mM; T = 25 ± 1 °C).

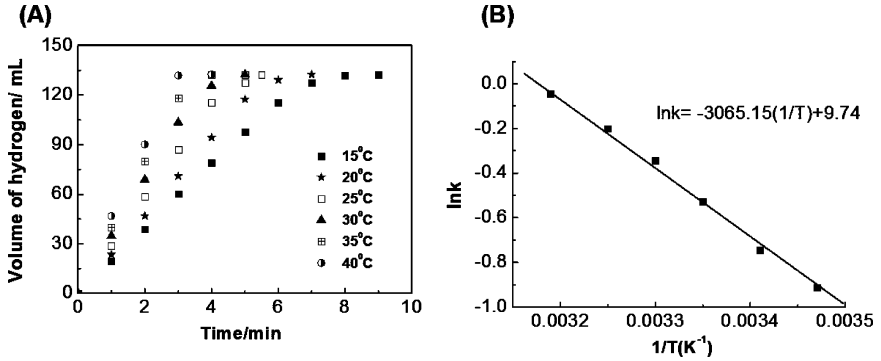

Figure 6. (A) Plot of time versus volume of hydrogen generated from methanolysis of AB catalyzed by $Co_{48}Pd_{52}/C$ catalyst at different temperatures and (B) Arrhenius plot of ln k versus $1/T$ ([AB] = 200 mM, [CoPd] = 3.6 mM).

Table 1. Catalysts Tested and Their Activity Comparison in Hydrogen Generation from the Methanolysis of AB

catalyst	metal/AB ratio (mol/mol)	maximum H_2/AB ratio (mol/mol)	completion time (min)	TOF (mol H_2 mol catalyst^{-1} min^{-1})	activation energy E_a (kJ mol^{-1})	ref
$RuCl_3$	0.000625	3.0	32	150		22
$RhCl_3$	0.02	3.0	1.5	100		22
$CoCl_2$	0.02	3.0	40	3.7		22
$NiCl_2$	0.02	3.0	51	2.9		22
$PdCl_2$	0.02	3.0	100	1.5		22
Pd/C	0.02	3.0	80	1.9		22
nano Cu@Cu_2O	0.15	1.8		0.16		34
nano Cu_2O	0.15	2.2		0.2		34
Co−Co_2B	0.2	3.0	2	7.5		35
Ni−Ni_3B	0.2	3.0	3	5.0		35
Co−Ni−B	0.2	3.0	1.5	10.0		35
PVP stabilized-Pd nanoclusters	0.005	3.0	27	22.3	35	33
zeolite-confined Rh(0) nanocluster	0.003	3.0	22	30	40 ± 2	23
MMT-immobilized Ru nanoparticle	0.003	3.0	11	90.9	23.8	6
$Co_{48}Pd_{52}/C$	0.027	3.0	4	27.7	25.5	this study

Figure 4A shows the plots of time versus volume of H_2 generated from AB methanolysis catalyzed by $Co_{48}Pd_{52}/C$ at different NP concentrations at 25 ± 1 °C. We can see that the catalyst can easily initiate the AB methanolysis, and a stoichiometric amount of H_2 (~67 mL, 3 mmol) is generated within less than 15 min. The higher the catalyst concentration is, the sooner the methanolysis is completed. Figure 4B is the plot of the H_2 generation rate versus the CoPd concentration in the logarithmic scale. The slope of 1.05 from the well-fitted line indicates that the methanolysis of AB catalyzed by the 7 nm $Co_{48}Pd_{52}/C$ catalyst is first-order with respect to the catalyst concentration, which is similar to what was reported on methanolysis of AB catalyzed by MMT/Ru,[6] zeolite-confined Rh,[23] and in situ-generated PVP-stabilized Pd nanoclusters.[33]

The H_2 generation rate was found to be independent of AB concentration (Figure 5). The nearly horizontal line (slope of

dx.doi.org/10.1021/cs300211y | ACS Catal. 2012, 2, 1290−1295

0.01) of H_2 generation rate versus AB concentration in logarithmic scale indicates that the NP-catalyzed methanolysis is zero-order with respect to the concentration of AB. This infers that in the methanolysis reaction, the adsorption of AB on the $Co_{48}Pd_{52}/C$ catalyst surface is a rate-limiting step. Our test is consistent with the report of Özkar on PVP-stabilized Pd NPs[33] but differs from that observed by Wang on MMT/Ru[6] and Ramachandranon on $RuCl_3$,[22] in which AB methanolysis follows first-order kinetics. The zero-order kinetics observed from our CoPd and the reported PVP-stabilized Pd catalysts seems to indicate that in the AB concentrations studied, the methanolysis mechanism is mainly dependent on the Pd component presented on the NP surface.

Figure 6 shows the plot of time versus the volume of H_2 generated during AB methanolysis at various temperatures. The values of the rate constant, k, were calculated from the slope of the linear part of each plot in part A to determine the activation energy. Part B shows the Arrhenius plot, from which the activation energy (E_a) for the methanolysis is calculated to be 25.5 kJ mol^{-1}. E_a and TOF values of all catalysts reported thus far for AB methanolysis are listed in Table 1. The value of our $Co_{48}Pd_{52}/C$ catalyst is comparable to the reported E_a for the methanolysis reaction of AB catalyzed by montmorillonite-immobilized Ru NPs (23.8 ± 1.2 kJ mol^{-1}). It is also close to the reported E_a for the hydrolysis of AB in the presence of Pt catalysts (21−23 kJ mol^{-1}).

Recyclability of the $Co_{48}Pd_{52}/C$ catalyst at room temperature was tested. After complete methanolysis of AB (64.0 mg, 2 mmol), the CoPd/C catalyst was kept in the reaction solution under ambient conditions, and another equivalent of AB was added to the reaction system. Figure 7A shows the conversion

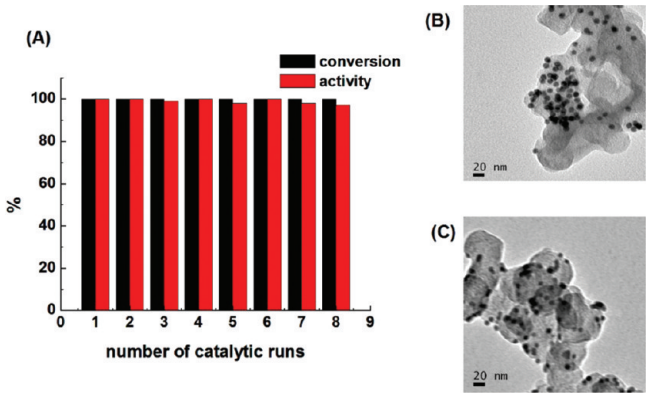

Figure 7. (A) Catalytic activity and conversion of AB versus the number of catalytic runs for the $Co_{48}Pd_{52}/C$ catalyst ([CoPd] = 3.6 mM, [AB] = 200 mM, T = 25 ± 1 °C). Catalytic activity (mL H_2/min) in the first run is set as 100%. TEM images of $Co_{48}Pd_{52}/C$ catalyst before (B) and after (C) eight catalytic runs.

of AB and the activity percentage change of the $Co_{48}Pd_{52}/C$ catalyst in subsequent AB methanolysis. The catalyst retains 98% of its initial catalytic activity at the eighth run. The slight decrease in catalytic activity at/after the eighth run is likely caused by the increase in the viscosity of the solution during the AB methanolysis. TEM images (shown in Figure 7B−C) prove that there is no significant change in either the NP size or its morphology during the test.

In summary, we have reported a unique solution phase synthesis of monodisperse 7 nm CoPd NPs with controlled compositions and studied their catalytic activity in hydrogen generation from the methanolysis of ammonia borane at room temperature. The CoPd NPs show the composition-dependent methanolysis at room temperature, with $Co_{48}Pd_{52}$ NPs being the most active. The kinetic studies on these $Co_{48}Pd_{52}/C$ catalysts reveal that the methanolysis is first-order with respect to the catalyst concentration and zero-order with respect to ammonia borane concentration. The activation energy and the total turnover frequency value for the methanolysis reaction is 25.5 kJ mol^{-1} and 27.7 mol of H_2·(mol of catalyst·min)$^{-1}$, respectively. Furthermore, the $Co_{48}Pd_{52}/C$ catalyst has also shown an excellent catalytic cycle life. The CoPd/C is promising in replacing Ru, Rh, and other noble metal components as an active catalyst for practical methanolysis of ammonia borane and for hydrogen generation.

EXPERIMENTAL METHODS

Chemicals. Cobalt(II) acetylacetonate (98%), palladium(II) bromide (99%), trioctylphosphine (90%), oleylamine (>70%), and ammonia borane (97%) were purchased from Sigma Aldrich and used as received. Methanol (99.5%) was purchased from Sigma Aldrich and dried by refluxing with magnesium turnings before use.

Synthesis of Monodisperse CoPd NPs. Under constant nitrogen flow, 0.35 mmol $Co(acac)_2$ (acac = acetylacetonate), 0.15 mmol $PdBr_2$, and 1.0 mL of TOP were mixed with 18 mL of OAm . The mixture was heated to 260 °C at a heating rate of 5 °C min^{-1}. The solution was kept at 260 °C for 1 h before it was cooled to room temperature. Next, 40.0 mL of isopropyl alcohol was added, and the product was separated by centrifugation at 8500 rpm for 8 min. The product was then dispersed in hexane. ICP−AES analysis revealed that the composition of the as-synthesized NPs was $Co_{48}Pd_{52}$. The alloy composition could be controlled by varying the ratio of $Co(acac)_2$ to $PdBr_2$.

Synthesis of CoPd/C Catalyst. A 15.0 mg portion of CoPd NPs was dispersed in 5.0 mL of hexane and 5.0 mL of acetone in a 20.0 mL glass vial and mixed with 45 mg of Ketjen carbon (surface area 800 m^2/ g) support. The mixture was sonicated for 1 h to ensure complete absorption of NPs onto the carbon support. After evaporation of hexane under a gentle nitrogen flow, the solid residue was suspended in 10.0 mL of methanol by sonication for 30 min to ensure uniform distribution.

Methanolysis of AB Catalyzed by CoPd/C Catalysts. The classic water-displacement method was employed in the study of the catalytic activity of the CoPd NPs/C catalysts toward methanolysis of AB. Before starting the catalytic activity test, a jacketed reaction flask (25 mL) containing a Teflon-coated stir bar was placed on a magnetic stirrer and thermostatted to 25.0 ± 1 °C by circulating water through its jacket from a constant temperature bath. Then, a buret filled with water was connected to the reaction flask to measure the volume of hydrogen gas evolved from the reaction. Next, 10.0 mL of methanol suspension of the catalyst was transferred into the reaction flask, and 64.0 mg (2 mmol, 200 mM) of AB was added into the catalyst solution at 800 rpm stirring rate. The volume of hydrogen gas evolved was measured by recording the displacement of the water level every 30s. The reaction was considered to cease when hydrogen gas generation was no longer observed. For a control experiment, 64.0 mg of AB and 45.0 mg Ketjen carbon was dispersed in 10.0 mL of methanol without any catalytic materials present in a temperature range of 15−40 °C. No hydrogen generation was observed in 12 h.

dx.doi.org/10.1021/cs300211y | ACS Catal. 2012, 2, 1290−1295

Catalyst Recyclability in the Methanolysis of AB. After the hydrogen generation reaction was completed, the as-synthesized CoPd/C catalysts were kept in the reaction solution under ambient conditions and another equivalent of AB (64 mg, 2 mmol) was added to the reaction system. The gas generation was monitored by volume changes in the buret. The process was repeated eight cycles.

Characterizations. Samples for transmission electron microscopy (TEM) and high-resolution TEM (HRTEM) analysis were prepared by depositing a single drop of diluted NP dispersion in hexane on amorphous-carbon-coated copper grids. Images were obtained by a JEOL 2010 TEM (200 kV) equipped with an energy-dispersive X-ray (EDX) analysis unit. The composition of the CoPd NPs was established by inductively coupled plasma−atomic emission spectroscopy. For ICP−AES analyses, the dried NPs were dissolved in warm aqua regia (~70 °C) for 30 min to ensure the complete dissolution of metal into the acid. The solution was then diluted with 2% HNO_3 solution. The measurements were carried out on a JY2000 Ultrace ICP−AES equipped with a JY-AS 421 auto sampler.

AUTHOR INFORMATION

Corresponding Author

*E-mails: (D.S.) sdaohua@xmu.edu.cn, (S.S.) ssun@brown.edu.

Notes

The authors declare no competing financial interest.

ACKNOWLEDGMENTS

The work was supported in part by Exxon Mobil (S.S.); the National Natural Science Foundation of China, Nos. 21036004 and 21106117 (D.S.); the Scientific and Technological Research Council of Turkey (TUBITAK) for 2214-Research fellowship program; and the METU-DPT-OYP program on the behalf of Ataturk University (Ö.M.).

REFERENCES

(1) Schlapbach, L.; Züttel, A. *Nature* **2001**, *414*, 353−358.
(2) Eberle, U.; Felderhoff, M; Schüth, F. *Angew. Chem., Int. Ed.* **2009**, *48*, 6608−6630.
(3) Marder, T. B. *Angew. Chem., Int. Ed.* **2007**, *46*, 8116−8118.
(4) Stephens, F. H; Pons, V.; Baker, R. T. *Dalton Trans.* **2007**, *25*, 2613−2626.
(5) Wang, P.; Kang, X. D. *Dalton Trans.* **2008**, *40*, 5400−5413.
(6) Dai, H. B.; Kang, X. D.; Wang, P. *Int. J. Hydrogen Energy* **2010**, *35*, 10317−10323.
(7) Chandra, M.; Xu, Q. *J. Power Sources* **2006**, *156*, 190−194.
(8) Xu, Q.; Chandra, M. *J. Alloys Compd.* **2007**, *446−447*, 729−732.
(9) Chandra, M.; Xu, Q. *J. Power Sources* **2007**, *168*, 135−142.
(10) Cheng, F.; Ma, H.; Li, Y.; Chen, J. *Inorg. Chem.* **2007**, *46*, 788−794.
(11) Clark, T. J.; Whittell, G. R.; Manners, I. *Inorg. Chem.* **2007**, *46*, 7522−7527.
(12) Yan, J. M.; Zhang, X. B.; Han, S.; Shioyama, H.; Xu, Q. *Angew. Chem., Int. Ed.* **2008**, *47*, 2287−2289.
(13) Kalidindi, S. B.; Indirani, B.; Jadirgar, B. R. *Inorg. Chem.* **2008**, *47*, 7424−7429.
(14) Metin, Ö.; Sahin, S.; Özkar, S. *Int. J. Hydrogen Energy* **2009**, *34*, 6304−6313.
(15) Basu, S.; Brockman, A.; Gagare, P.; Zheng, Y.; Ramachandran, P. V.; Delgass, W. N. *J. Power Sources* **2009**, *188*, 238−243.
(16) Metin, Ö.; Özkar, S. *Energy Fuels* **2009**, *23*, 3517−3526.
(17) Rakap, M.; Özkar, S. *Int. J. Hydrogen Energy* **2010**, *35*, 1305−1312.
(18) Metin, Ö.; Mazumder, V.; Özkar, S.; Sun, S. H. *J. Am. Chem. Soc.* **2010**, *132*, 1468−1469.
(19) Metin, Ö; Özkar, S.; Sun, S. H. *Nano Res.* **2010**, *3*, 676−684.
(20) Yan, J. M..; Zhang, X. B.; Akita, T.; Haruta, M.; Xu, Q. *J. Am. Chem. Soc.* **2010**, *132*, 5326−5327.
(21) Lo, C. F.; Karan, K.; Davis, B. R. *Ind. Eng. Chem. Res.* **2007**, *46*, 5478−5484.
(22) Ramachandran, P. V.; Gagare, P. D. *Inorg. Chem.* **2007**, *46*, 7810−7817.
(23) Caliskan, S.; Zahmakıran, M.; Özkar, S. *Appl. Catal., B* **2010**, *93*, 387−394.
(24) Erdogan, H.; Metin, Ö.; Özkar, S. *Catal. Today* **2011**, *170*, 93−98.
(25) Metin, Ö.; Özkar, S. *Int. J. Hydrogen Energy* **2011**, *36*, 1424−1432.
(26) Yao, C. F.; Zhuang, L.; Cao, Y. L.; Hi, X. P.; Yang, H. X. *Int. J. Hydrogen Energy* **2008**, *33*, 2462−2467.
(27) Yang, X. J.; Cheng, F. Y.; Liang, J.; Tao, Z. L.; Chen, J. *Int. J. Hydrogen Energy* **2009**, *34*, 8785−8791.
(28) Burda, C.; Chen, X. B.; Narayanan, R.; El-Sayed, M. A. *Chem. Rev.* **2005**, *105*, 1025−1102.
(29) Sun, D. H.; Mazumder, V.; Metin, Ö.; Sun, S. H. *ACS Nano* **2011**, *5* (8), 6458−6454.
(30) Mazumder, V.; Chi, M.; Mankin, M.; Liu, L.; Metin, Ö.; Sun, D.; More, K. L.; Sun, S. *Nano Lett.* **2012**, *12*, 1102−1106.
(31) Demirci, U. B.; Garin, F. J. *Alloys Compd.* **2008**, *463*, 107−111.
(32) Greeley, J.; Jaramillo, T. F.; Bonde, J.; Chorkendorff, I.; Nørskov, J. K. *Nat. Mater.* **2006**, *5*, 909−913.
(33) Erdogan, H.; Metin, Ö.; Özkar, S. *Phys. Chem. Chem. Phys.* **2009**, *44*, 10519−10525.
(34) Kalidindi, S. B.; Sanyal, U.; Jagirdar, B. R. *Phys. Chem. Chem. Phys.* **2008**, *10*, 5870.
(35) Kalidindi, S. D.; Vernekar, A. S.; Jadirgar, B. R. *Phys. Chem. Chem. Phys.* **2009**, *11*, 770−775.